JOURNAL OF CATALYSIS **146**, 601–607 (1994)

NOTE

On the Microstructure of the Coprecipitated Ni–Al_2O_3 Catalysts

Nickel–alumina catalysts are commonly used in steam reforming (1) and methanation (2) reactions. Due to the high reaction temperatures (700–1000 K), especially for the steam reforming, a high thermostability of the Ni–Al_2O_3 is required. In a previous study of impregnated and model Ni–Al_2O_3 catalysts it has been shown that after reduction in hydrogen the metallic nickel crystallites are covered by nickel aluminate shells (3). The presence of the nickel aluminate shells explains the high stability of the metal phase towards sintering under working conditions (3). The carbon monoxide adsorption study on these materials showed that the nickel crystallites are not completely encapsulated (4). Both bridged and on-top Ni–CO complexes were observed.

A number of previous studies on the structure and properties of nickel–alumina catalysts refer to materials prepared by the coprecipitation method (5–13). Two different models of catalyst structures have been proposed. Alzamora *et al.* (7) considered the presence of alumina crystallites on the surface of the metal phase, preventing their coalescence. Puxley *et al.* (8) suggested that all alumina of the catalyst is enclosed within nickel, forming a "para crystalline" nickel phase. In a recent study of the coprecipitated Ni–Al_2O_3 catalyst Zielinski (14) suggested that the reduced catalyst consists of nickel crystallites and amorphous nonstoichiometric NiO–Al_2O_3 residues. The NiO–Al_2O_3 residues are believed to be present in two different localizations, i.e. (i) as clusters situated between/on nickel crystallites and (ii) inclusions encapsulated within large nickel crystallites (14).

Direct information about structure and location of different Ni-species present in the Ni–Al_2O_3 catalysts can be obtained from high-resolution and analytical electron microscopy studies. For coprecipitated Ni–Al_2O_3 only one electron microscopy investigation exists (9). The aim of this study is to recognize in greater detail the chemical microstructures on coprecipitated Ni–Al_2O_3 catalysts. It will be shown that the metallic nickel phase is covered with nickel aluminate shells after reduction in hydrogen. The decoration of the nickel crystallites with $NiAl_2O_4$ is considered to be crucial for the high sinter stability of the Ni–Al_2O_3 catalysts (3).

The investigations were carried out on 97.5 and 85% wt.% Ni–Al_2O_3 catalysts prepared by coprecipitation from Ni $(NO_3)_2$ and $NaAlO_2$ aqueous solution (14, 15). After washing and drying the precipitates were calcined in air at 673 K for 2 h, reduced in H_2 at 773 K for 2 h, and then passivated in Ar at 473 K.

To obtain a high fraction of catalyst fragments sufficiently thin for EM observation the Ni–Al_2O_3 specimens were ground to a fine powder and dispersed ultrasonically on standard 3-mm grids covered with thin amorphous carbon foils. No solvents were used in this procedure. Part of the TEM study was carried out with a Philips EM 420 T transmission electron microscope operated at 120 eV and equipped with an energy-dispersive X-ray analyzer (EDX). High-resolution electron microscopy examinations were performed in a Philips CM 20 Ultra Twin electron microscope operated at 200 kV and providing a 0.19 nm point resolution. It has been checked that the (220) lattice planes of gold (d = 0.144 nm) can be imaged in this instrument.

Electron micrographs of the 97.5 and 85% Ni–Al_2O_3 samples are shown in Figs. 1a and 1b. Selected area diffraction patterns obtained from these specimens are shown in Figs. 2a and 2b. The analysis of the diffractograms shows the presence of metallic nickel and nickel aluminate (Table 1). Closer inspection of Fig. 1 and corresponding electron diffraction patterns (Fig. 2) reveals differences in the size of the nickel crystallites. In the case of the 97.5% Ni–Al_2O_3 specimens the formation of very large nickel crystallites is observed (Fig. 1a). High-resolution observation of the 97.5% Ni–Al_2O_3 sample shows the presence of large, well-crystallized nickel particles covered with a material which gives rise to a weaker contrast compared to metallic nickel and is assumed to be nickel aluminate (Fig. 3). The presence of moiré fringes ("M") indicates the crystalline character of nickel aluminate. The large Ni crystallite shown in Fig. 3 consists of some smaller crystallites which are twinned or connected with incoherent boundaries. The presence of such incoherent boundaries creates interface defects and gives rise to misfit strain energy. In addition to very large nickel crystallites (Fig. 3) the 97.5% Ni–Al_2O_3 specimen shows the presence of smaller nickel crystallites separated by nickel aluminate phase (Fig. 4). Analysis of the lattice plane distances indicates the presence of the crystalline $NiAl_2O_4$ phase (Fig. 4). Figure 5 depicts a typical electron micrograph taken from the 85% Ni–Al_2O_3 specimen and reveals that the nickel crystallites are much smaller, as

0021-9517/94 $6.00

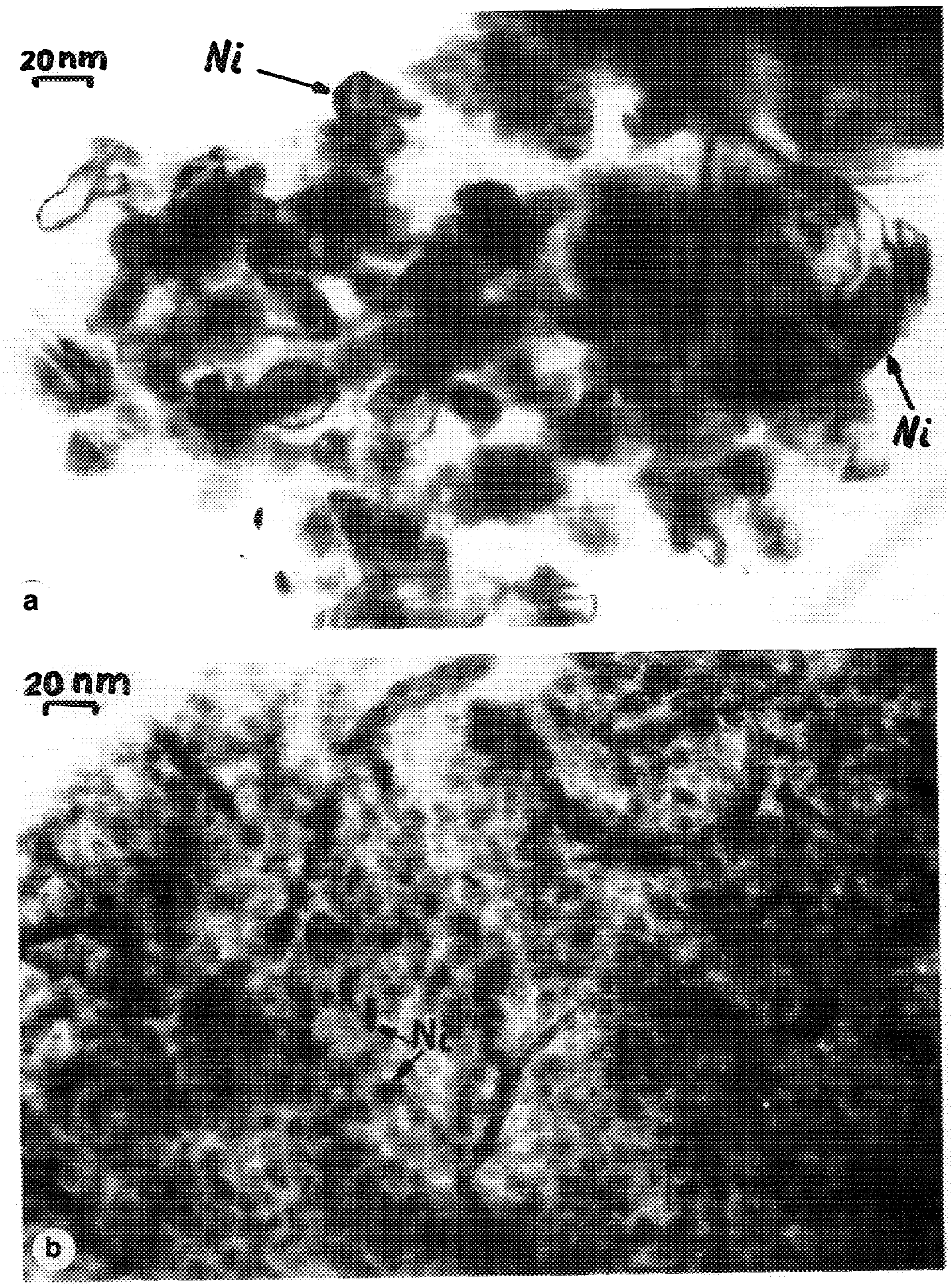

FIG. 1. Electron micrographs of the Ni–Al_2O_3 specimen after reduction in H_2 at 773 K. (a) 97.5% Ni–Al_2O_3; (b) 85% Ni–Al_2O_3. The Ni crystallites were identified using a dark field image technique.

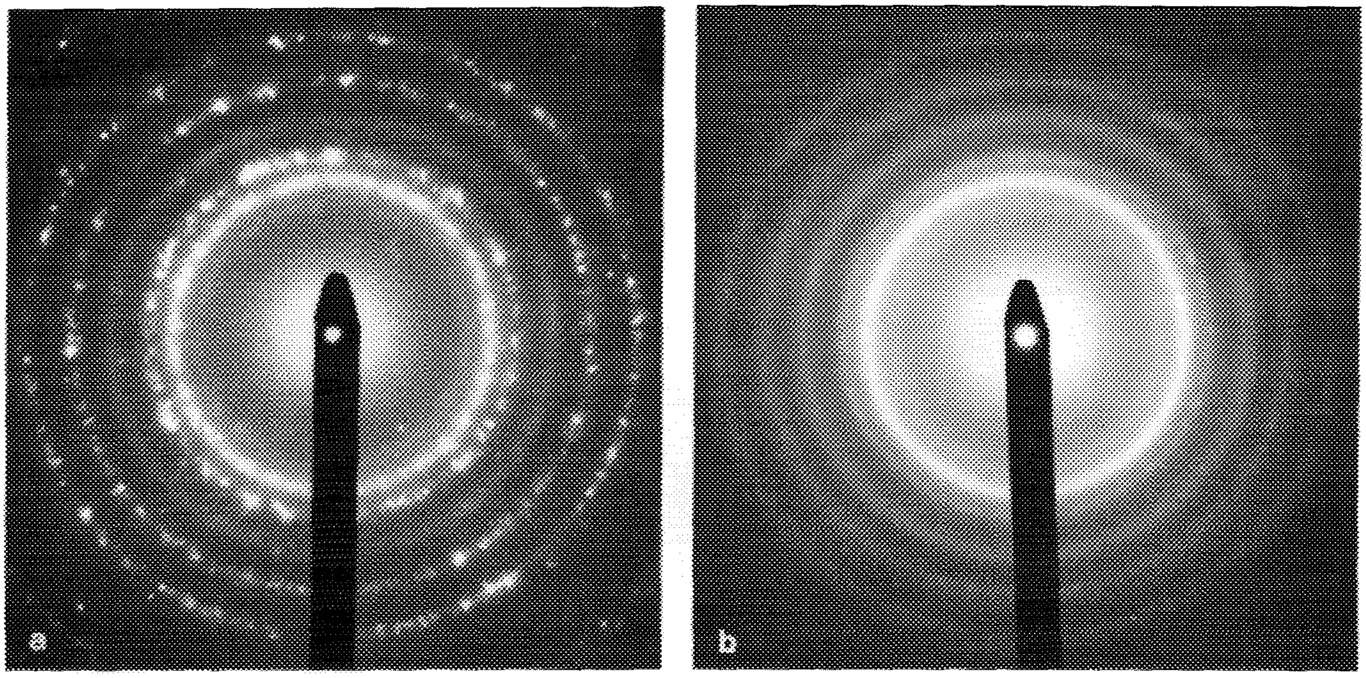

FIG. 2. Selected area diffraction pattern obtained for (a) the 97.5% Ni–Al_2O_3 sample and (b) the 85% Ni–Al_2O_3 sample.

observed in the case of the 97.5% Ni–Al_2O_3 specimen. The presence of partially crystalline pin-shaped material is visible. Analysis of the lattice plane distances (0.28 and 0.24 nm) indicates the presence of either nickel aluminate or γ-alumina phase.

The electron diffraction investigation of coprecipitated Ni–Al_2O_3 catalysts shows the presence of the nickel aluminate phase after reduction at 773 K. High-resolution observations reveal that the nickel aluminate covers the nickel crystallites. The decoration of the metallic nickel phase with the nickel aluminate is similar to that previously observed for impregnated and model Ni–Al_2O_3 catalysts (3). It can be stated that the high thermal stability of both impregnated and coprecipitated catalysts is guaranteed by the nickel aluminate shells formed on the nickel crystallites. The question arises whether after reduction in hydrogen the gas molecules has access to the active nickel phase. The CO adsorption study on the impregnated Ni–Al_2O_3 catalysts showed that the nickel aluminate shells do not hamper the accessibility of the metal surface for reacting molecules (4). This indicates that the nickel aluminate shells exhibit voids or pores guaranteeing access of the gas molecules to the nickel surface (4). A preliminary carbon monoxide adsorption study on coprecipitated Ni–Al_2O_3 catalysts reduced at 773 K demonstrates their ability to adsorb CO. Bands which are characteristic for linearly (ca. 2080 cm^{-1}) and bridged (ca. 1950 cm^{-1}) bonded CO on nickel metal appear (19). Murthy and Swamy (18) have recently shown that the reduction of $NiAl_2O_4$ at temperatures >723 K leads to a partial reduction of the spinel. XPS studies revealed the presence of metallic nickel species (18). According to these results and previous studies by Ross *et al.* (6) and Al-Ubaid and Wolf (12) one should consider the possibility that some adsorptive and catalytic active sites are also present on/in the nickel aluminate shells covering the metallic nickel crystallites. Future adsorption studies aiming to discriminate between different nickel species present in the copre-

TABLE 1

Measured Interplanar Distances *d* (nm) for the Reduced Ni–Al_2O_3 Samples in Comparison with Interplanar Distances for Nickel (16) and Nickel Aluminate (17)

Ni		Ni–Al_2O_3 97.5%	Ni–Al_2O_3 85%	$NiAl_2O_4$	
I/I_0	*d* (nm)	*d* (nm)	*d* (nm)	*d* (nm)	I/I_0
		0.282	—	0.2846	20
		0.243	0.243	0.2427	100
100	0.2034	0.203	0.202	0.2015	65
42	0.1762	0.175	0.175		
		—	—	0.164	8
		—	—	0.154	30
		0.144	0.144	0.142	60
21	0.1246	0.125	0.125	0.1227	10

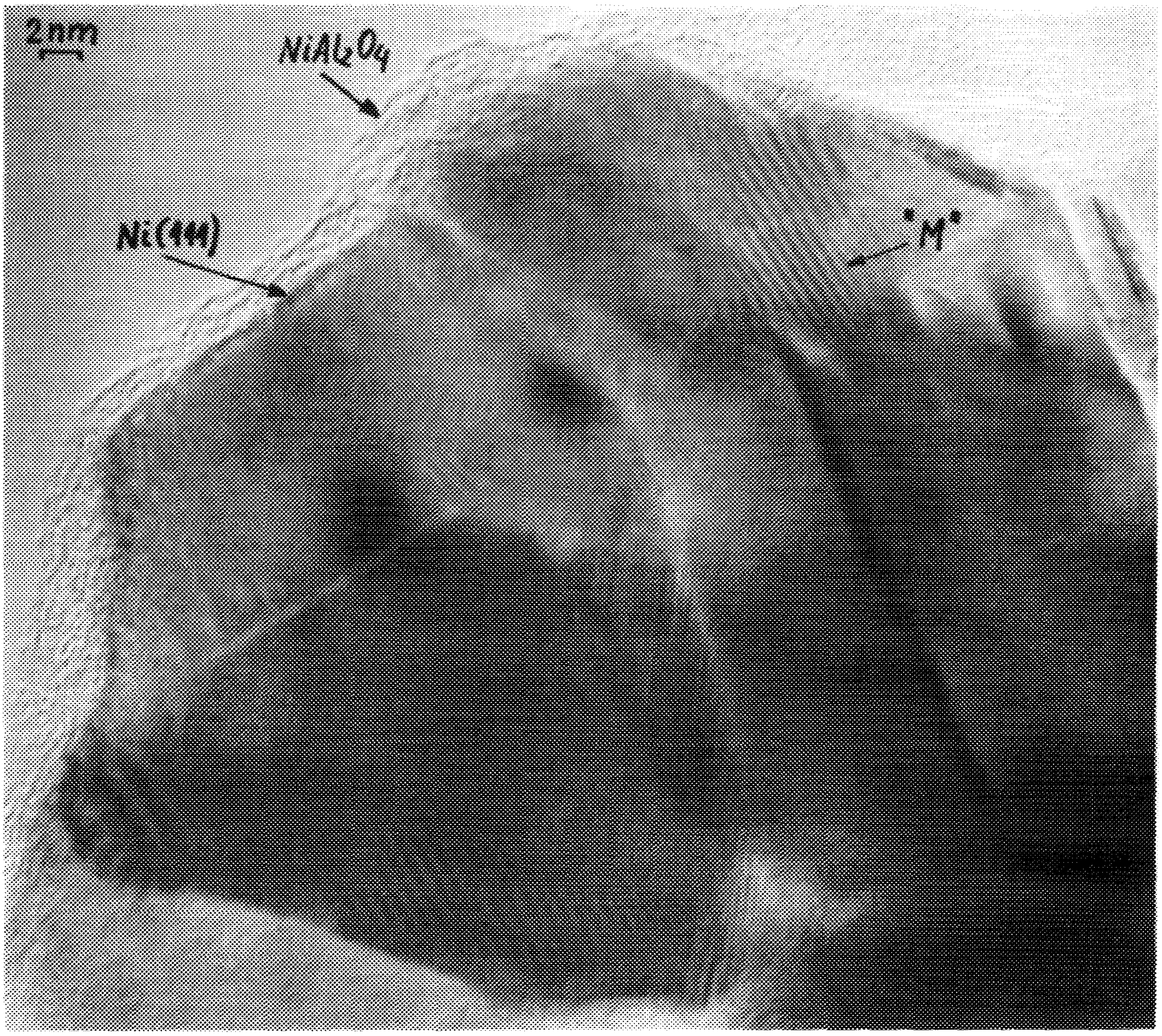

FIG. 3. HRTEM image of the 97.5% Ni–Al_2O_3 specimen.

cipitated Ni–Al_2O_3 catalysts after reduction at different temperatures would be suitable as was demonstrated for impregnated Ni–Al_2O_3 contacts (4).

Electron diffraction and high-resolution electron microscopy studies of coprecipitated Ni–Al_2O_3 catalysts have shown the formation of the nickel aluminate shells on the metallic nickel crystallites, which is responsible for the high sinter stability of these materials. These results are in principle in agreement with the model proposed by Zielinski (14). The nickel aluminate shell phase is, however, crystalline and present either as a layer covering the metal nickel crystallites or as aggregates situated in the vicinity of the nickel crystallites. The nickel aluminate exhibits voids and pores that guarantee access of the gas molecules to the nickel surface (4, 19). On the basis of other results (6, 12, 18) it can be expected that the catalytically active nickel species on/in the nickel aluminate shells exist.

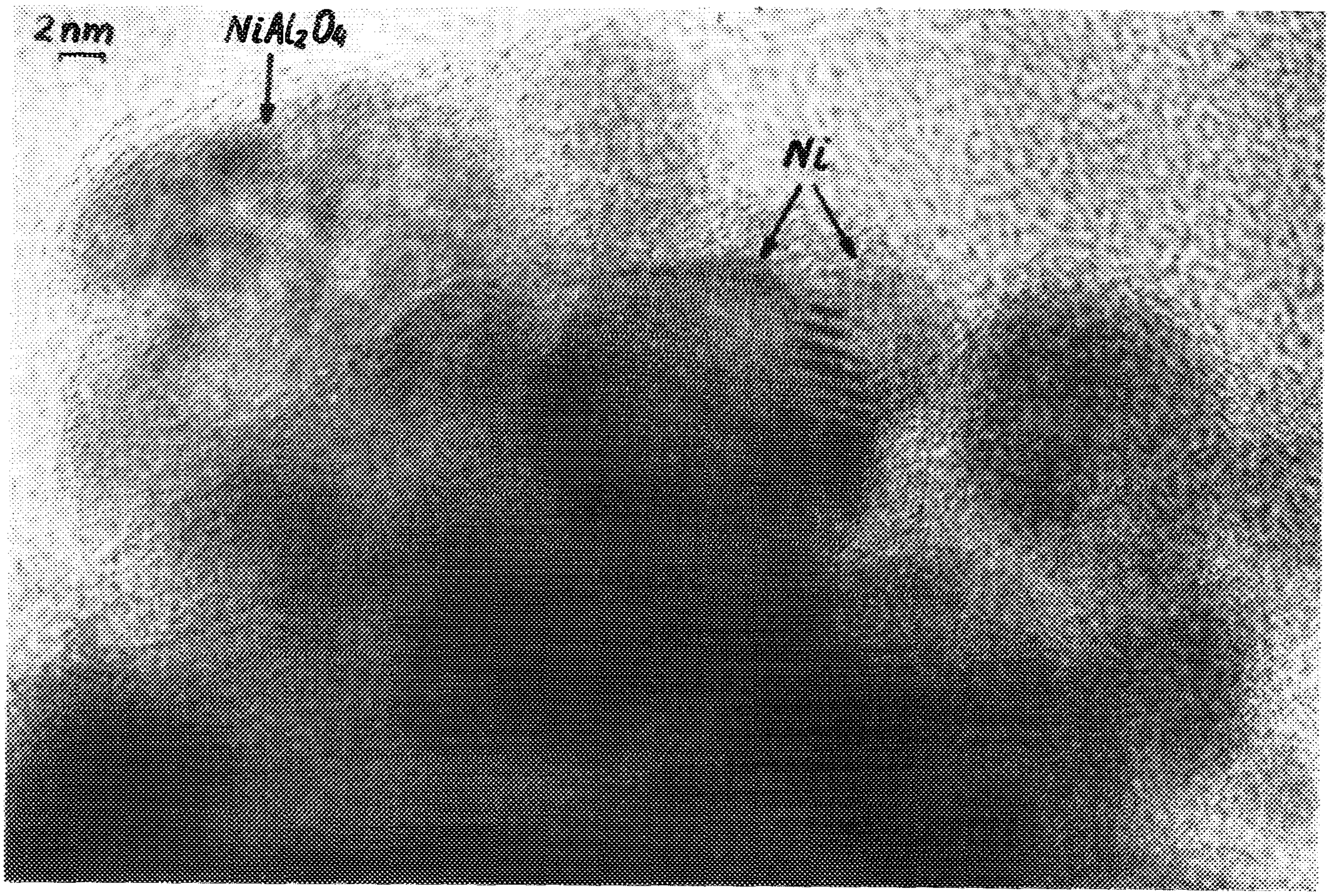

FIG. 4. High-magnification image of the metallic nickel and nickel aluminate crystallites (97.5% Ni–Al_2O_3).

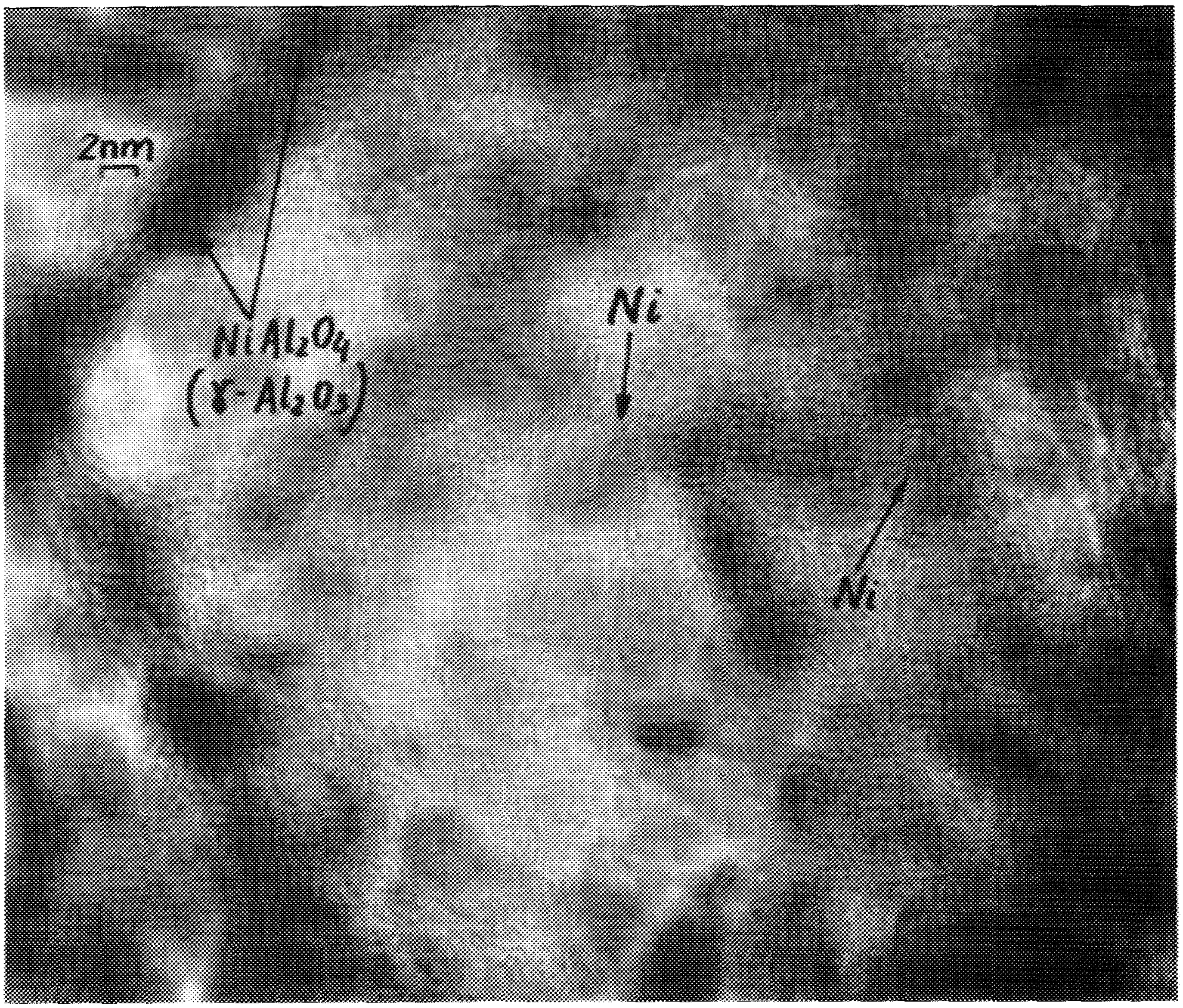

FIG. 5. HRTEM image of the 85% Ni–Al_2O_3 sample.

ACKNOWLEDGMENTS

We thank Dr. J. Zielinski for providing us with samples of the 97.5% and 85% Ni–Al_2O_3 catalysts. We are grateful to Professor N. I. Jaeger for valuable contributions and a critical reading of the manuscript.

REFERENCES

1. Rostrup-Nielsen, J. R., *in* "Catalysis: Science and Technology" (J. R. Anderson and M. Boudart, Eds.), Vol. 5, p. 1. Springer, Berlin, 1984.
2. Vannice, M. A., *in* "Catalysis: Science and Technology" (J. R. Anderson and M. Boudart, Eds.), Vol. 3, p. 139. Springer, Berlin, 1982.
3. Lamber, R., and Schulz-Ekloff, G., *Surf. Sci.* **258,** 107 (1991).
4. Kubelkova, L., Novakova, J., Jaeger, N. I., and Schulz-Ekloff, G., *Appl. Catal. A* **95,** 87 (1993).
5. Doesburg, E. B. M., Orr, S., Ross, J. R. H., and van Reijen, L. L., *J. Chem. Soc., Chem. Commun.*, 734 (1977).
6. Ross, J. R. H., Steel, M. C. F., and Zeini-Isfahani, Z., *J. Catal.* **52,** 280 (1978).
7. Alzamora, L. E., Ross, J. R. H., Kruissink, E. C., and van Reijen, L. L., *J. Chem. Soc., Faraday Trans. I* **77,** 665 (1981).
8. Puxley, D. C., Kitchener, J. J., Kromodromos, C., and Parkyns, N. D., *in* "Preparation of Catalysts III" (G. Poncelot, G. Grange, and P. A. Jacobs, Eds.), p. 237. Elsevier, Amsterdam, 1983.
9. Doesburg, E. B. M., Hakvoort, G., Scharper, H., and van Reijen, L. L., *Appl. Catal.* **7,** 85 (1983).
10. Doesburg, E. B. M., de Korte, P. H. M., Scharper, H., and van Reijen, L. L., *Appl. Catal.* **11,** 155 (1984).

11. Lansik Rotgerink, H. G. J., Bosch, H., van Ommen, J. G., and Ross, J. R. H., *Appl. Catal.* **27,** 41 (1986).
12. Al-Ubaid, A., and Wolf, E. E., *Appl. Catal.* **40,** 73 (1988).
13. Clause, O., Rebours, B., Morlen, E., Trifiro, F., and Vaccari, A., *J. Catal.* **133,** 231 (1992).
14. Zielinski, J., *Appl. Catal.* A94 (1993) 107.
15. Zielinski, J., *J. Mol. Catal.* **83,** 197 (1993).
16. Powder Diffraction File, Joint Committee on Powder Diffraction, International Center for Diffraction Data, Swarthmore, PA 1987, Card. 4-0850.
17. Powder Diffraction File, Joint Committee on Powder Diffraction, International Center for Diffraction Data, Swarthmore, PA 1987, Card. 10-339.
18. Murthy, I. A. P. S., and Swamy, C. S., *J. Mat. Sci.* 28 (1993) 1194.
19. Unpublished results.

Ryszard Lamber
Günter Schulz-Ekloff

Institut für Angewandte und Physikalische Chemie
Universität Bremen
28334 Bremen, Germany

Received September 3, 1993; revised December 1, 1993